Supplementary Material to

Silencing of cryptic prophages in *Corynebacterium glutamicum*

Eugen Pfeifer[1], Max Hünnefeld[1], Ovidiu Popa[2], Tino Polen[1], Dietrich Kohlheyer[1], Meike Baumgart[1], and Julia Frunzke[1,*]

Supplementary Tables

Table S1. Strains and plasmids used in this study.

Strains	Relevant characteristics	Reference
E. coli		
DH5α	*supE44* Δ*lacU169* (φ80*lacZ*DM15) *hsdR17 recA1 endA1 gyrA96 thi-1 relA1*, strain used for cloning procedures	Invitrogen
BL21(DE3)	F^-*ompT hsdS*$_B$(r_B^- m_B^-) *gal dcm* BL21(DE3), protein production host	(1)
S3974	Derivate of K-12 (CGSC #6300), F^-, λ^-, *rph*$^+$ *ilvG*$^+$	(2)
T221	S3974 Δ*hns*$_{FRT,,}$ *E. coli* strain used for complementation studies of Δ*hns* phenotype	(3)
M. tuberculosis		
H37Rv	wild-type laboratory strain, DNA used as PCR template	ATCC 25618
C. diphtheriae		
ATCC 27010	wild-type laboratory strain, DNA used as PCR template	DSM 44123
C. amycolatum		
PAP 272	wild-type, genomic DNA was used for PCR as template	DSM 44737

C. glutamicum		
ATCC 13032	Biotin-auxotrophic wild type	(4)
WT::*cgpS-strep*	Derivative of ATCC 13032 with genomic exchange of the *cgpS* gene to *cgpS-strep*, encoding a C-terminal Strep-tag fusion.	This study
ATCC 13032 ΔCGP3	ATCC 13032 with in-frame deletion of prophage CGP3 (cg1890-cg2071)	(5)
WT::P_{lys} *-eyfp*	Derivative of ATCC 13032 containing the prophage reporter P_{lys}-*eyfp* integrated into the intergenic region of cg1121-cg1122	(6)
Plasmids		
pAN6	*Kan*^{R}*; C. glutamicum*/*E. coli* shuttle vector for gene expression under control of the *tac* promoter; (P_{tac}, *lacI*^{q}*, pBL*$_1$ *ori*$V_{C.g.}$, pUC18 *ori*$V_{E.c.}$)	(7)
pAN6-*cgpS*	Derivative of pAN6 containing the *cgpS* gene	This study
pAN6-*cgpS-Strep*	Derivative of pAN6 containing the *cgpS* gene without stop codon encoding a C-terminal Strep-tag fusion	This study
pAN6-*N-cgpS*	Derivative of pAN6 containing the first 65 amino acids of the *cgpS* gene	This study
pAN6-*N-cgpS-Strep*	Derivative of pAN6 containing the first 65 amino acids of the *cgpS* gene fused C-terminally to a Strep-tag coding region	This study
pAN6-*lsr2-N-M.tub*	Derivative of pAN6 containing the first 58 amino acids of the *lsr2* gene (Rv3597c) of *Mycobacterium tuberculosis* H37Rv	This study
pAN6-c*gpS-N-C.amyc*	Derivative of pAN6 containing the first 66 amino acids of the homologous *cgpS* gene (CORAM0001_2081) of *Corynebacterium amycolatum* DSM 44373	This study
pAN6-*cgpS-N-C.diph*	Derivative of pAN6 containing the first 59 amino acids of the homologous *cgpS* gene (DIP2266) of *Corynebacterium diphtheriae* DSM 44123	This study

pAN6-*alpA-eyfp*	Derivative of pAN6 containing a *alpA-eyfp* fusion	This study
pK19*mobsacB*	Kan^R; plasmid for allelic exchange in *C. glutamicum*; (pK18 *ori*$V_{E.c.}$, *sacB*, *lacZ*α)	(8)
pK19mobsacB-*cgpS-Strep*	Derivative of pK19*mobsacB* containing the *cgpS-Strep* construct for the allelic exchange of the native *cgpS* gene to a C-terminally strep-tagged version in the chromosome of *C. glutamicum*.	This study
pK18*mobsacB*-	Kan^R; plasmid for integration of foreign DNA into the intergenic region between cg1121-cg1122 (*ori*$V_{E.c.}$, *sacB*, *lacZ*α).	(5)
pEC-XC99E	*cat*$_I$, *lacI*^{q}, P_{trc}, *rrnB* (T1 and T2), *oriV*$_{E.c}$, *per* and *repA* (pGA1)$_{C.g.}$. *E. coli – C. glutamicum* shuttle and expression vector conferring chloramphenicol resistance.	(9)
pEC-XC99E-*cgpS-mcherry*	Derivative of pEC-XC99E containing the *cgpS* gene cloned upstream of the *mcherry* gene under control of the *tac* promoter.	This study

Table S2. Oligonucleotides used in this study for cloning, qPCR and affinity chromatography. Bold sequences represent the overlapping sequences needed for Gibson assembly (10). Restriction sites are underlined.

Application	Oligo-nucleotide	Sequence (5´→ 3´) and properties	Comment
pK19*mobsacB-cgpS-strep*	LF_cgpS_pK19_fw	**CCTGCAGGTCGACTCTAGAG** CTGGTCGTCTGTGTAGCTAC	PCR product contains an overlapping sequence to *Bam*HI-digested pK19*mobsacB* plasmid
	LF_cgpS_rv	GTCCATAGTCCTAACCAATCATGTAA	
	cgpS_strep_fw	**GATTGGTTAGGACTATGGAC** ATGGCCATTATTCAGTCGGTC	PCR product contains an overlapping sequence to the left flank of *cgpS* (PCR product above)
	cgpS_strep_rv	TTACTTCTCGAACTGTGGGTG	
	RF_cgpS_fw	**CACCCACAGTTCGAGAAGTAA** GAGCCCTGTGGAGAATTGTTG	PCR product contains overlapping sequences to *cgpS-strep* and to an *Eco*RI-digested pK19*mobsacB* plasmid
	RF_cgpS_pK19_rv	**AAAACGACGGCCAGTGAATT** ACGCGGCGACCTCATC	
	Cgps_indel-fw	GGACATTATCACCCAACCACAC	Oligonucleotides to verify the correct integration of *cgpS-strep*
	CgpS_indel_rv	CAAGGAATCGTTTACCTATATCGAG	
			Restriction enzyme
pAN6 with the coding regions for the N-terminal parts of the CgpS/Lsr2 homologs	C.a.fw	GCGC <u>CATATG</u> ATGGCACGCCGCGAACTAAT	*Nde*I
	C.a.fw	CGCG <u>CCCGGG</u> ATGGCACGCCGCGAACTAAT	*Sma*I
	C.a.N.rv	GCGC <u>GCTAGC</u> CTATACAACCGTGCTGTGATCAATAG	*Nhe*I
	C.a.rv	GCGC <u>GGATCC</u> CTAGTTAGCGCTCTCGTACTTTTC	*Bam*HI
	C.d.fw	CGCG <u>CATATG</u> ATGGCACGTCGTGAAATC	*Nde*I
	C.d.fw	CGCG <u>CCCGGG</u> ATGGCACGTCGTGAAATC	*Sma*I
	C.d.N.rv	GCGC <u>GCTAGC</u> CTAGTGCGCTTTTTCTATGAAGGG	*Nhe*I
	C.d.rv	GCGC <u>GGATCC</u> TTAGCGCTTGGTGGACTTAAG	*Bam*HI
	M.t.fw	GCGC <u>CATATG</u> ATGGCGAAGAAAGTAACCGTC	*Nde*I
	M.t.fw	CGCG <u>CCCGGG</u> ATGGCGAAGAAAGTAACCGTC	*Sma*I
	M.t.N.rv	GCGC <u>GCTAGC</u> CTAGACGCGACGGCCCG	*Nhe*I
	M.t.rv	GCGC <u>TCTAGA</u> TCAGGTCGCCGCGTG	*Xba*I

pAN6 *cgpS*/ *cgpS-strep*/ *cgpS*-N/ *cgpS*-N-*strep*	cgps_fw	CGCGC CATATG ATGGCCATTATTCAGTCGGTCG	*Nde*I
	cgps_strep_rv	CGCGC GCTAGC TTCGAAAGGAATGCCTTCTTTTTC	*Nhe*I
	cgps_rv	CGCGC GAATTC TTA TTCGAAAGGAATGCCTTC	*Eco*RI
	cgpS_n_rv	CGCGC GCTAGC TTA CTGGCGTGCAGATTCCTC	*Nhe*I
	cgpS_n_strep _rv	CGCGC GCTAGC CTGGCGTGCAGATTCCTC	*Nhe*I
pAN6-*alpA-eyfp*	alpA_OL_pAN 6_fw	**TGCAGAAGGAGATATACATA** ATGGCTCAAAAACAGGACACGAC	PCR product contains overlapping sequences to *Nde*I and *Eco*RI-digested pAN6 plasmid
	eYFP-OL_pAN6_rv	**AAAACGACGGCCAGTGAATT** TTATCTAGACTTGTACAGCTCGTCC	
pEC-XC99E-*cgpS-mcherry*	PcgpS-pEC-fw	**GCGGTATTTCACACCGCATATG** CTGGTCGTCTGTGTAGCTAC	PCR product contains overlapping sequences to *Nde*I -digested pEC-XC99E plasmid and to *mcherry*
	cgpS-rv-OL-mcherry	**CTCGCCCTTGCTCACCAT** TTCGAAAGGAATGCCTTCTTTTTCG	
	mcherry_fw	ATGGTGAGCAAGGGCGAG	PCR product contains an overlapping sequence to *PstI* -digested pEC-XC99E plasmid
	mCherry_rv_O L	**AACAGCCAAGCTTGCATGCC** TTACTTGTACAGCTCGTCCATGC	
Application	**Oligo-nucleotide**	**Sequence (5´→ 3´)**	**Comments**
qPCR (circular phage DNA and reference gene)	Phage-LC-for	CCCACGTTCACCCCACAAACG	
	Phage-LC-rev	CTAAAATGAAGCCATCGCGACC	
	ddh-LC-for	ACGTGCTGTTCCTGTGCATGG	
	ddh-LC-rev	GCTCGGCTAAGACTGCCGCT	
Affinity chromatography with P_{alpAC}	PalpAC-Biotin-Tag fw	*GAGGAGTCGTCGATGTGGAGACC* TCGCACTCAATAATGCGGTGG	Asterisks highlight the biotin labelled sequences
	Biotin-oligo	*GAGGAGTCGTCGATGTGGAGACC*	
	PalpAC rv	GCGCATACGCACATTACGC	

Table S3. Oligonucleotides used for the generation of DNA fragments for EMSA experiments.

Oligonucleotide	Sequence (5´→ 3´) and properties	Product length (bp)	GC content of product (%)
gntK-Prom-fw	ATGGTGGCGTCATGCTCGGCCG	560	49.3
gntK-Prom-rv	GGATTTGCCGCAGCCAGAAACGC		
cg0150fw	GGGGTAATAAGACAAAACAGTGGG	500	39.6
cg0150rv	TAGAAATCAGCGACAACCATGCTTC		
cg0421fw	GGATACTTTCTGTTTTGGTTGGTC	500	41.5
cg0421rv	GAAATTACCAAGATGCACCACCTC		
cg0432fw	CCTTTTCTAGACAAGACCTGATC	500	42.0
cg0432rv	ACCAACGACGTCGGATTAGG		
cg0718fw	ATAAGTCATGGTTCAACCTCGG	500	44.0
cg0718rv	CCTAAAACGACACCATCTCAAAAG		
cg0726fw	TACCACTTGCCTTTGTAGCGTTC	500	46.0
cg0726rv	ACTTGGAAACCGGCAGCAAG		
cg1028fw	TGGTCAGCGCAGCGAC	500	50.3
cg1028rv	AAGTTGAGTCTTGGGCCGG		
cg1517fw	GTATGACCAAATGGGACGAAGG	500	42.0
cg1517rv	GATAAGCCACTCAACCACCAAAC		
cg2782fw	GACGCTGAGAAGGACTACG	500	49.5
cg2782rv	TTGAAGGTATCTCCGACAGCAAC		
cg2805fw	AAGAAGGCTGAGTTTAGTGGGG	500	44.8
cg2805rv	AGAAGACGTCCAAAATCCCGTC		
cg3060fw	CAAAATCAATGCGAGAGCGAAG	500	44.0
cg3060rv	CTGCAGAGCTGAAATTATCGAC		
cg3304fw	GGATAACTTCCCCACAATTGAC	500	47.7
cg3304rv	AAGCGTGCCATTGTTCTCCC		
cg1951fw	CTCTATTGGCTCTTAATGGTCAATTAC	500	33.4
cg1951rv	GCCTCTTAAAGCACAGTTATTGCG		
cg1966fw	GCTCAGTATCAATGTCGTCACC	500	36.3
cg1966rv	GTCGAAGTGGTGTCGTTATTTAGG		
cg2023fw	GCACCACCAACAAGTGCC	500	40.7
cg2023rv	TGGGAGCATTTCACTGCACG		
cg1977fw	GTTCTAAACATAAGGAACGCGC	500	39.1
cg1977rv	CGATGGTGCAGTGACCATG		
cg1936fw	CATCGCTCATTGTTACTTAATTACCC	500	36.0
cg1936rv	CCTGAAGAATTTGCTCAGCCG		
cg1940fw	CCATAGTCAAGATTCCCAATCAAC	500	39.5
cg1940rv	GATTCAGGTGATGTAGCGCTG		
cg1917fw	CCTGTAGCCTGCGACGTTAA	500	42.2
cg1917rv	GTGCACCGGTAGCCATAATAG		
cg1895fw	TCACGGGTGGAATCGGAG	500	38.3
cg1895rv	GCTTGGATCATCTGAACAGAGTG		
cg2014fw	AGCGTCAATCGGAATCTGCG	500	40.7
cg2014rv	CAGTTGCGCTAGATAAGCGAG		
cg1890fw	GCGACAAACAAATAGATCAGCTG	500	41.8
cg1890rv	GGGGTTTATTACCTGCCTGC		

Table S4. Results of the ChAP-Seq experiment. The 90 identified regions are evaluated regarding their peak width, peak maxima and area. Furthermore, the regions are classified into three categories as described in Figure S3. Genes within the CGP3 region are highlighted in green.

Table S5. Impact of CgpS countersilencing on the *C. glutamicum* transcriptome. CGP3 prophage genes are highlighted in green**.** ORFs exhibiting are more than two-fold altered mRNA ratio (of >2 or < 0.5, *p*-value <0.05) are shown.

Table S6. PSI-BLAST results of CgpS. e-value was set <= 0.005 across several orders of the phylum Actinobacteria and phages as annotated in the NCBI database (http://www.ncbi.nlm.nih.gov/).

Supplementary Figures

A

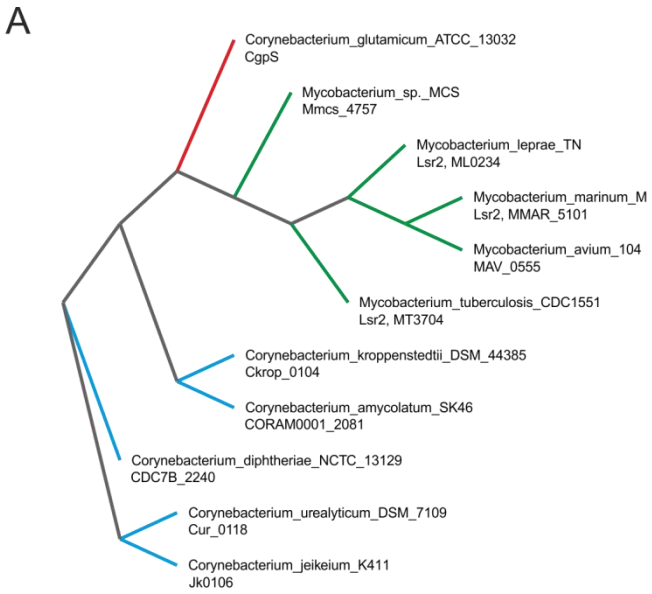

B

	***Corynebacterium glutamicum* ATCC 13032**	**100**	**27.52**	**25.66**	**25.96**	**27.27**	**25.45**	**21.55**	**23.42**	**24.76**	**24.55**	**21.1**
1	*Mycobacterium spec.* MCS	27.52	100	87.93	90.09	87.83	86.09	28.45	27.35	30.77	36.61	34.82
2	*Mycobacterium marinum* M	25.66	87.93	100	93.69	94.87	94.02	26.89	29.91	28.57	40.18	35.71
3	*Mycobacterium avium* 104	25.96	90.09	93.69	100	91.82	91.82	27.27	27.93	30.3	36.45	35.19
4	*Mycobacterium tuberculosis* CDC1551	27.27	87.83	94.87	91.82	100	92.31	28.45	31.03	28.85	40.54	34.23
5	*Mycobacterium leprae* TN	25.45	86.09	94.02	91.82	92.31	100	27.59	28.45	28.85	37.84	35.14
6	*Corynebacterium kroppenstedtii* DSM 44385	21.55	28.45	26.89	27.27	28.45	27.59	100	41.32	39.81	40.35	38.6
7	*Corynebacterium amycolatum* SK46	23.42	27.35	29.91	27.93	31.03	28.45	41.32	100	40.74	41.74	43.48
8	*Corynebacterium diphtheria* NCTC 13129	24.76	30.77	28.57	30.3	28.85	28.85	39.81	40.74	100	44.86	49.06
9	*Corynebacterium urealyticum* DSM 7109	24.55	36.61	40.18	36.45	40.54	37.84	40.35	41.74	44.86	100	53.51
10	*Corynebacterium jeikeium* K411	21.1	34.82	35.71	35.19	34.23	35.14	38.6	43.48	49.06	53.51	100

Figure S1: CgpS orthologs. A. Phylogenetic tree based on the multiple sequence alignments of CgpS/Lsr2 homologs of selected *Corynebacteria* (*C. kroppenstedtii*, *C. amycolatum*, *C. diphteriae*, *C. urealyticum*, *C. jeikeium*), and *Mycobacteria* (*M. tuberculosis*, *M. spec.*, *M. leprae*, *M. marinum*, *M. avium*). Alignments were performed using Clustal Omega (11) with standard configurations. Data for phylogenetic tree were derived from alignments and visualized using tree vector (12). Analysis indicates that CgpS displays a higher sequence identity to mycobacterial Lsr2 proteins than to the corynebacterial orthologs.

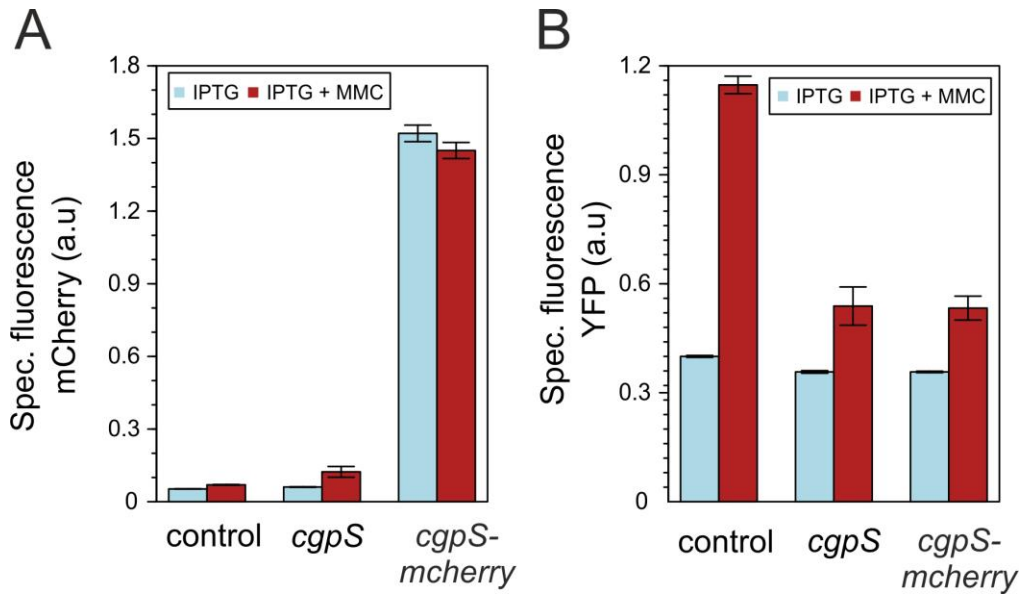

Figure S2: Silencing of CGP3 prophage induction. A and B. Phage reporter cells (WT::P_{lys}-*eyfp*) were transformed with pAN6, pAN6-*cgpS* and pAN6-*cgpS-mcherry* and were cultivated in CGXII with 50 µM IPTG and in the presence or absence of 0.6 µM MMC. The mCherry (A) and eYFP (B) fluorescence as well as backscattered light were measured in the BioLector® microcultivation system and were used to calculate the specific fluorescence. The specific fluorescence after 20 h of cultivation is shown. The data represent average values from three biological replicates including the standard deviation.

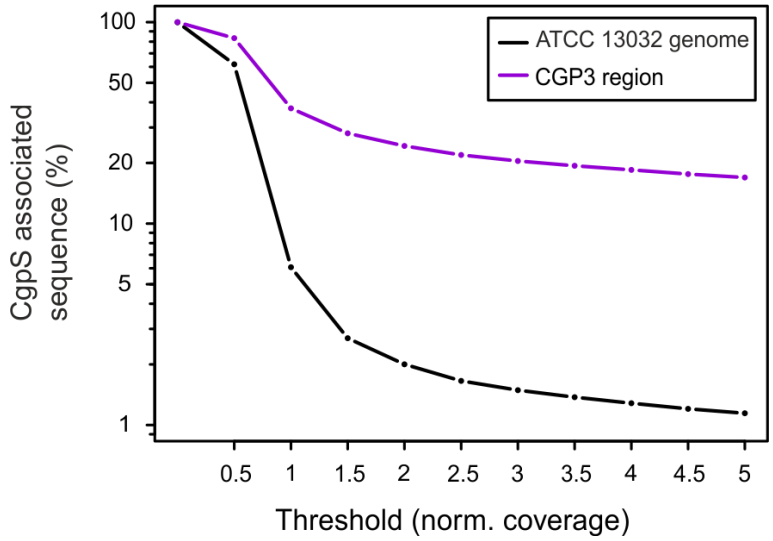

Figure S3: Threshold variation of the CgpS ChAP-Seq data. Based on mean normalized coverage values which were obtained by ChAP-sequencing experiments, thresholds were varied to validate its impact on the estimated binding of CgpS to the CGP3 region and to the entire genome of ATCC 13032. Based on this analysis, bound regions showing a threshold T >3 were considered as CgpS targets in this study (20.46% of CGP3 and 1.49% of the genome).

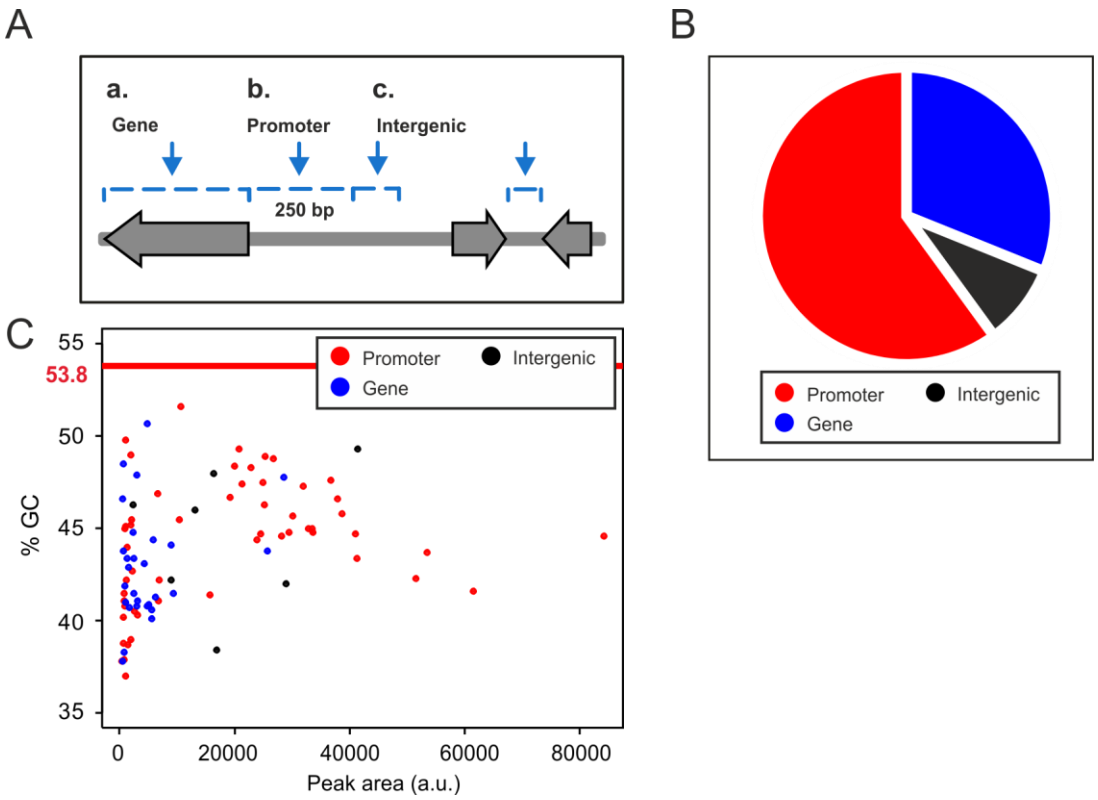

Figure S4: **Genomic distribution of CgpS binding sites within genes, promoters or intergenic regions. A.** The 90 regions bound to CgpS were classified into three categories: i. Binding sites within open reading frames (genes), ii. 250 bp upstream of translational start or according to published transcription start sites (promoter regions), and, iii. intergenic regions. **B**. Distribution of the 90 CgpS-bound genomic regions. Overall, 60% of the peaks are located in promoter regions and 31% within genes. Only 9% are assigned to intergenic regions**. C**. The %GC content of the regions were plotted against peak areas. Red line illustrates average GC content of *C. glutamicum* ATCC 13032, which is about 53.8% (13). Interestingly, a trend to higher peak areas was observed for promoter regions in comparison to intergenic regions or ORFs.

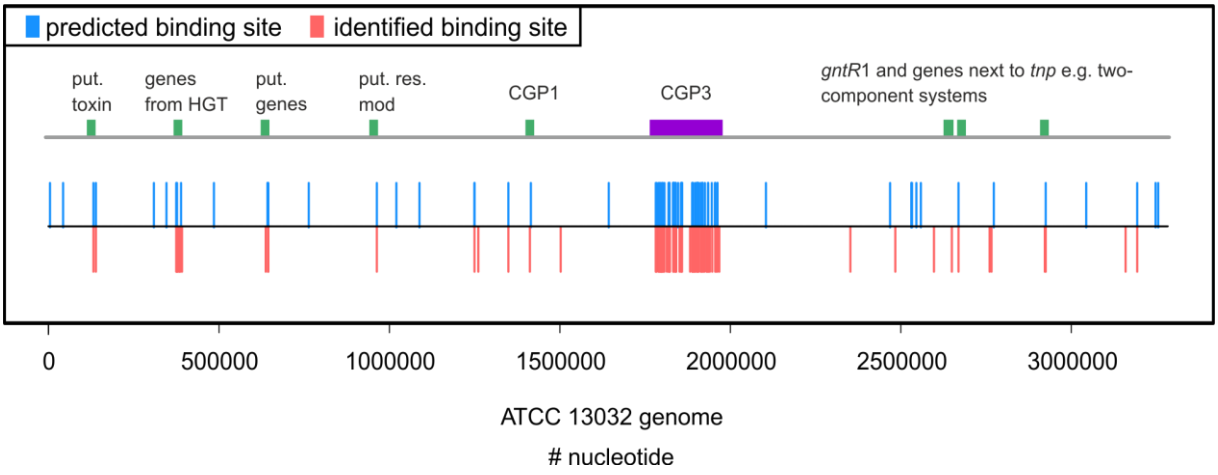

Figure S5: Comparison of predicted and experimentally identified CgpS binding sites. The DNA binding motif derived from ChAP-Seq results (Fig. 3C) was checked for further hits in the genome of ATCC 13032 using FIMO (14). Here, 90 positions exhibiting highest probability (p-Values: $2.7 \cdot 10^{-10}$ – $2.3 \cdot 10^{-6}$) (in blue) were compared with the 90 experimentally identified binding sites acquired by ChAP-Seq binding studies (in red). Potential CgpS site within the CGP3 region (purple boxes) and outside (green boxes) are highlighted. Correlation between experimentally identified and predicted CgpS binding sites ~75 %.

A Upstream of CGP3

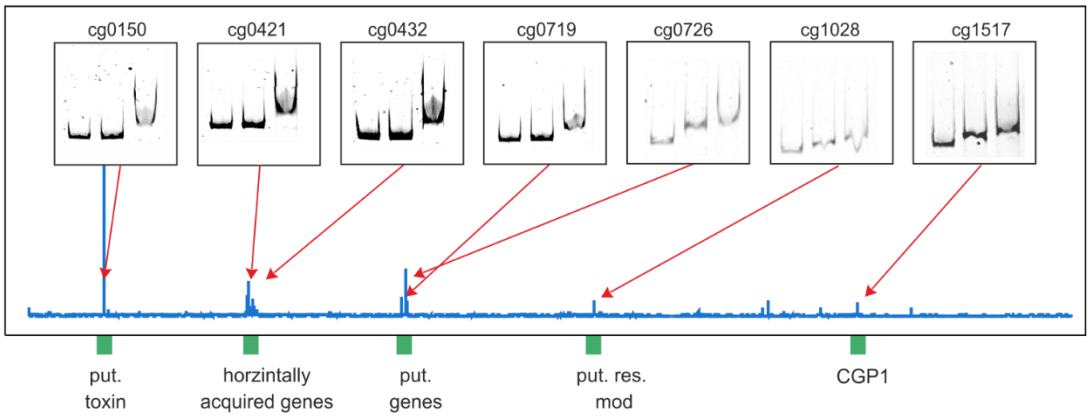

B

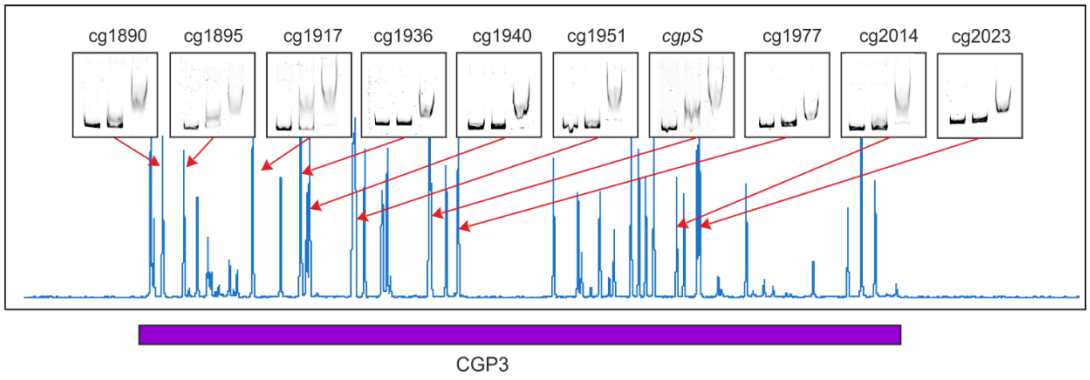

Downstream of CGP3

C

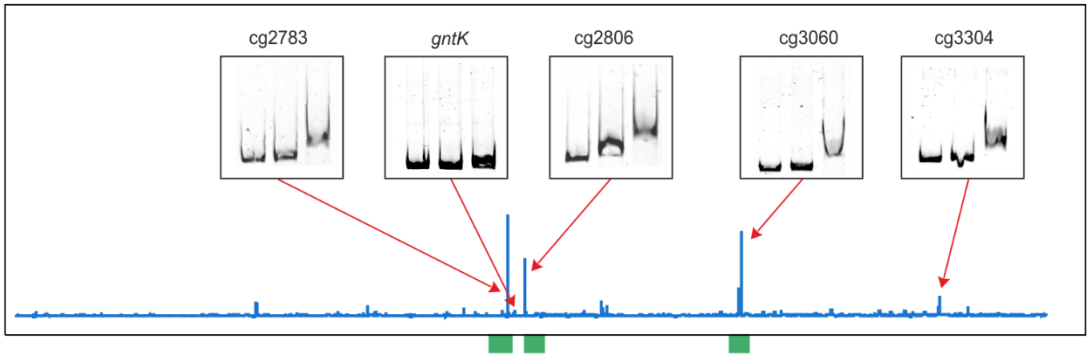

*gntR*1 and genes next to tnp e.g. two-component systems

D

cg0150	putative transcriptional regulator, Fic/Doc- family	**cg1936**	putative secreted protein, CGP3 region
cg0421	*wzx*, putative translocase involved in export of a cell surface polysaccaride	**cg1940**	putative secreted protein, CGP3 region
cg0432	putative lipopolysaccharide modification acyltransferase	**cg1951**	*tnp*14a, transposase fragment, CGP3 region
cg0719	*crtYe*, C50 carotenoid cyclase, terpenoid synthesis	**cg1966**	*cgpS*, Lsr2-like protein, CGP3 region
cg0726	putative secreted lipoprotein	**cg1977**	putative secreted protein, CGP3 region
cg1028	putative restriction modification system: methylase (EC:2.1.1.72)	**cg2014**	hypothetical protein, CGP3 region
cg1517	putative secreted protein, CGP1 region	**cg2023**	putative membrane protein, CGP3 region
cg1890	*alpC*, actin like protein, CGP3 region	**cg2783**	*gntR1*, gluconate-responsive repressor
cg1895	putative secreted protein, CGP3 region	**cg2806**	putative membrane protein
cg1917	hypothetical protein, CGP3 region	**cg3060**	*cgtS6*, two-component sensor kinase
		cg3304	*dnaB*, replicative DNA helicase

Figure S6: *In vitro* binding studies of CgpS to its putative target sites. Electrophoretic mobility shift assays (EMSAs) were performed with purified CgpS-Strep protein and 21 putative target DNA regions derived from ChAP-Seq data (Fig. 3). Green boxes indicate regions outside of CGP3 and the purple box sites within the CGP3 region. All tested DNA fragments had a size of about 500 bp and were chosen 250 bp up and downstream of the peak maxima, which were detected by the ChAP-Seq analysis. Overall, eleven candidate regions were chosen outside of CGP3 ((**A**) seven upstream and (**C**) four downstream of CGP3) and ten sites within the CGP3 region (**B**). In all lanes 90 ng DNA (12-14 pM) were incubated without (lane 1) or with increasing amounts of CgpS protein (lane 2: 1 µM and lane 3: 2 µM). The promoter region of *gntK* (560 bp) was used as a negative control. Annotations und potential functions of the bound regions are listed in **D**.

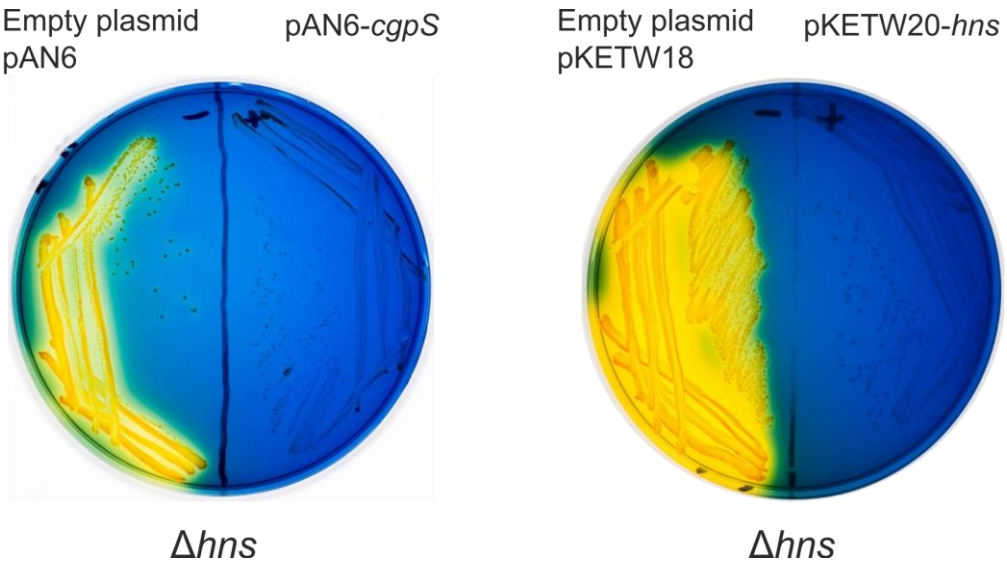

Figure S7: Complementation studies of a *E. coli* K-12 Δ*hns* strain with *cgpS* cloned into the overexpression plasmid pAN6. Cells were grown on bromothymol blue salicin indicator plates as described in Dole et al., 2002 (15). *E. coli* cells lacking *hns* were transformed with the empty plasmid pAN6, pAN6-cgpS or with the empty plasmid pKETW18 or pKETW20 carrying *hns*. Plates were incubated at 37°C overnight. Complementation is based on the utilization of salicin. Salicin can be used as carbon source if the *bgl* operon is expressed. This operon is repressed by H-NS in the wild type situation. Thus, in the absence of H-NS, salicin is metabolized leading to a decrease of the pH resulting in a colour shift from blue to yellow. Complementation of the Δ*hns* phenotype was achieved by expressing either *hns* or *cgpS* suggesting a similar function of both proteins.

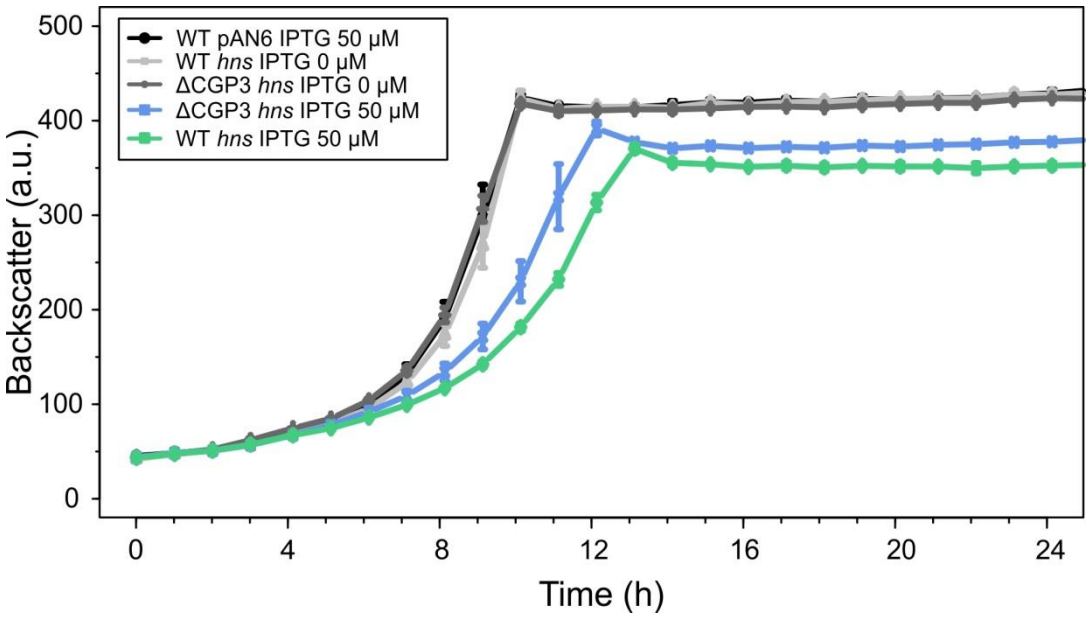

Figure S8: Overexpression of *hns* in *C. glutamicum* strains. H-NS encoding gene located on the overexpression plasmid pAN6 was overexpressed in the prophage reporter strain WT::P_{lys}-*eyfp* and in the ΔCGP3 strain. Cells were cultivated in CGXII minimal medium and *hns* expression was induced with 50 µM IPTG. The data represent average values of three biological replicates including the standard deviation.

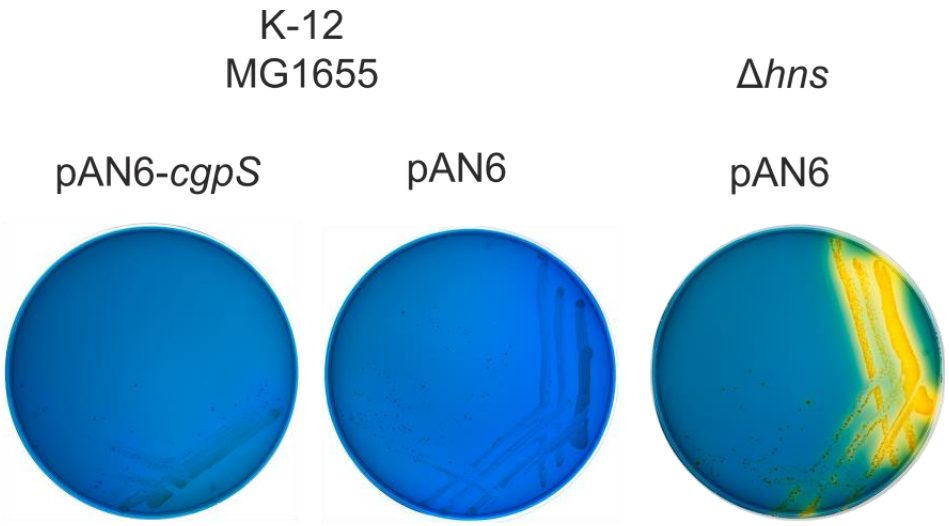

Figure S9: *cgpS* overexpression in *E. coli* wild type cells. To verify whether CgpS is interfering with the function of H-NS in its native host, *E. coli* K-12 MG1655 wild type cells were transformed with the pAN6-*cgpS* plasmid. Cells were streaked on bromothymol blue salicin indicator plates (15) supplemented with 100 µM IPTG. As control, the wild type strain and a Δ*hns* mutant were transformed with the empty plasmid pAN6. The obtained results suggest that heterologous *cgpS* expression is not able to counteract H-NS silencing at the *bgl* promoter when compared to a mutant lacking the *hns* gene. However, it needs to be highlighted that the resulting *E. coli* strain expressing the *cgpS* gene (left plate) showed a significant growth defect in comparison to the empty vector controls (middle and right).

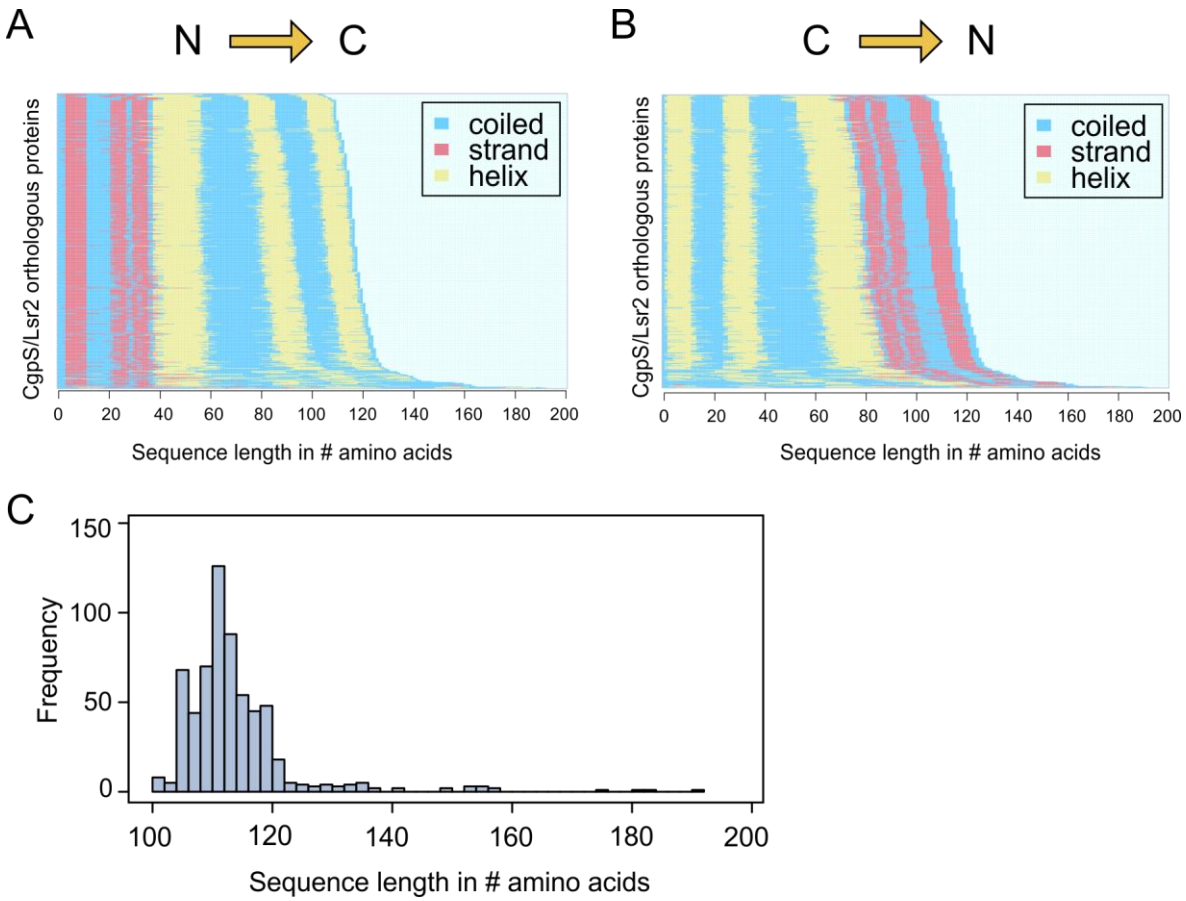

Figure S10. Bioinformatic analysis of CgpS related proteins. A PSI-BLAST search on CgpS homologs with an *e*-value of 0.005 was conducted and achieved 5230 hits (Table S6). 1920 sequence are individual and can be assigned to 863 taxonomical units; 618 of these can be allocated to bacteria or phages. Secondary structure predictions of the 618 sequences are shown in direct comparison in N->C (**A**) and C->N (**B**) orientation. The increasing length of the amino acid sequences entails distortet matches in secondary structure prediction and hence for a better overview the two possibilites are shown. **C.** Histogramm of the 618 sequences ordered according to their amino acid sequence length. The maximum of this distribution is located around 110 amino acids.

Supplementary Videos

Video S1: Time lapse video of a *C. glutamicum* microcolony under standard conditions (without IPTG, control). Cells of the prophage reporter strain ATCC 13032::P_{lys}-*eyfp* carrying the countersilencing plasmid pAN6-N-*cgpS* were cultivated in microfluidic chambers (16) in standard minimal medium (CGXII with 2% (w/v) glucose, 25 µg·ml kanamycin for 20 h without IPTG). The video shows the first 12 h of the cultivation.

Video S2: Time lapse video of the effect of CgpS countersilencing (150 µM IPTG) on prophage activation. The same reporter strain (Video S1) was grown in the presence of 150 µM IPTG inducing the expression of the truncated CgpS protein (aa 1-65) covering its oligomerization domain. The video shows the first 16.5 h of the experiment.

References

1. Studier, F.W. and Moffatt, B.A. (1986) Use of Bacteriophage-T7 Rna-Polymerase to Direct Selective High-Level Expression of Cloned Genes. *J Mol Biol*, **189**, 113-130.
2. Venkatesh, G.R., Koungni, F.C.K., Paukner, A., Stratmann, T., Blissenbach, B. and Schnetz, K. (2010) BglJ-RcsB Heterodimers Relieve Repression of the *Escherichia coli bgl* Operon by H-NS. *J Bacteriol*, **192**, 6456-6464.
3. Stratmann, T., Pul, U., Wurm, R., Wagner, R. and Schnetz, K. (2012) RcsB-BglJ activates the *Escherichia coli* leuO gene, encoding an H-NS antagonist and pleiotropic regulator of virulence determinants. *Mol Microbiol*, **83**, 1109-1123.
4. Kinoshita, S., Udaka, S. and Shimono, M. (1957) Studies on the amino acid fermentation - Part I. Production of L-glutamic acid by various microorganisms. *J Gen Appl Microbiol*, **50**, 331-343.
5. Baumgart, M., Unthan, S., Rückert, C., Sivalingam, J., Grünberger, A., Kalinowski, J., Bott, M., Noack, S. and Frunzke, J. (2013) Construction of a prophage-free variant of *Corynebacterium glutamicum* ATCC 13032 for use as a platform strain for basic research and industrial biotechnology. *Appl Environ Microbiol*, **79**, 6006-6015.
6. Helfrich, S., Pfeifer, E., Krämer, C., Sachs, C.C., Wiechert, W., Kohlheyer, D., Nöh, K. and Frunzke, J. (2015) Live cell imaging of SOS and prophage dynamics in isogenic bacterial populations. *Mol Microbiol*, **98**, 636-650.
7. Frunzke, J., Engels, V., Hasenbein, S., Gätgens, C. and Bott, M. (2008) Co-ordinated regulation of gluconate catabolism and glucose uptake in *Corynebacterium glutamicum* by two functionally equivalent transcriptional regulators, GntR1 and GntR2. *Mol Microbiol*, **67**, 305-322.
8. Schäfer, A., Tauch, A., Jager, W., Kalinowski, J., Thierbach, G. and Pühler, A. (1994) Small Mobilizable Multipurpose Cloning Vectors Derived from the *Escherichia-Coli* Plasmids Pk18 and Pk19 - Selection of Defined Deletions in the Chromosome of *Corynebacterium-Glutamicum*. *Gene*, **145**, 69-73.
9. Kirchner, O. and Tauch, A. (2003) Tools for genetic engineering in the amino acid-producing bacterium Corynebacterium glutamicum. *J Biotechnol*, **104**, 287-299.
10. Gibson, D.G., Young, L., Chuang, R.Y., Venter, J.C., Hutchison, C.A. and Smith, H.O. (2009) Enzymatic assembly of DNA molecules up to several hundred kilobases. *Nat Methods*, **6**, 343-U341.
11. Sievers, F., Wilm, A., Dineen, D., Gibson, T.J., Karplus, K., Li, W., Lopez, R., McWilliam, H., Remmert, M., Soding, J. *et al.* (2011) Fast, scalable generation of high-quality protein multiple sequence alignments using Clustal Omega. *Mol Syst Biol*, **7**, 539.
12. Pethica, R., Barker, G., Kovacs, T. and Gough, J. (2010) TreeVector: Scalable, Interactive, Phylogenetic Trees for the Web. *Plos One*, **5**.
13. Kalinowski, J., Bathe, B., Bartels, D., Bischoff, N., Bott, M., Burkovski, A., Dusch, N., Eggeling, L., Eikmanns, B.J., Gaigalat, L. *et al.* (2003) The complete *Corynebacterium glutamicum* ATCC 13032 genome sequence and its impact on the production of L-aspartate-derived amino acids and vitamins. *J Biotechnol*, **104**, 5-25.
14. Grant, C.E., Bailey, T.L. and Noble, W.S. (2011) FIMO: scanning for occurrences of a given motif. *Bioinformatics*, **27**, 1017-1018.
15. Dole, S., Kühn, S. and Schnetz, K. (2002) Post-transcriptional enhancement of *Escherichia coli bgl* operon silencing by limitation of BglG-mediated antitermination at low transcription rates. *Mol Microbiol*, **43**, 217-226.
16. Grünberger, A., Probst, C., Helfrich, S., Nanda, A., Stute, B., Wiechert, W., von Lieres, E., Nöh, K., Frunzke, J. and Kohlheyer, D. (2015) Spatiotemporal Microbial Single-Cell Analysis Using a High-Throughput Microfluidics Cultivation Platform. *Cytometry*, **87A**, 1101-1115.